RSC Advances

ROYAL SOCIETY
OF CHEMISTRY

www.rsc.org/advances

1   **Preparation of M/γ-Al$_2$O$_3$ sorbents and their desulfurization performance**

2   **in hydrocarbons**

3   Junjie Liao, Yashan Wang, Liping Chang, Weiren Bao[*]

4   State Key Laboratory Breeding Base of Coal Science and Technology Co-founded by Shanxi

5   Province and Ministry of Science and Technology, Taiyuan University of Technology, Taiyuan

6   030024, P.R. China

7   **Abstract**: M/γ-Al$_2$O$_3$ sorbents with different metals (Ag, Cu, Ni, Zn) as the active component

8   loaded on γ-Al$_2$O$_3$ support were prepared by incipient wetness impregnation method, and their

9   adsorption behavior for thiophene was investigated. The results show that all those metals can

10   obviously promote the desulfurization activity of the prepared sorbents, and Ag is the best one.

11   And then silver was selected to modify γ-Al$_2$O$_3$ with different loading amount, and the

12   desulfurization behavior of Ag/γ-Al$_2$O$_3$ series sorbents in thiophene-benzene solution was

13   evaluated. It was found that the silver content has a significant impact on desulfurization

14   efficiency, and the A15 sorbent with 13.7 wt% silver has the best adsorption desulfurization

15   performance. XRD results show that the simply Ag^0 is the main active component in

16   Ag/γ-Al$_2$O$_3$ sorbent. SEM/EDS and BET characterizations show that the specific surface area

17   and pore volume decrease obviously when silver loading amount is more than 13.7wt%,

18   because of the agglomeration of silver. The desulfurization mechanism of Ag/γ-Al$_2$O$_3$ sorbent

19   was explored by using thiophene which has both a conjugated pi bond and sulfur,

20   tetrahydrothiophene which has sulfur but no conjugated pi bond, benzene which has a

21   conjugated pi bond but no sulfur, cyclohexane which has no conjugated pi bonds or sulfur as

22   the model compounds. The desulfurization efficiencies of A15 sorbent in thiophene-benzene,

[*] Corresponding author: Weiren Bao Tel/Fax:+86 351 6010482

E-mail: baoweiren@tyut.edu.cn

23   thiophene-cyclohexane, thiophene-tetrahydrothiophene-benzene and

24   thiophene-tetrahydrothiophene-cyclohexane solutions were compared. The results indicate

25   that the thiophene adsorption on Ag/γ-Al$_2$O$_3$ sorbent is mainly dominated by two kinds of

26   connection between thiophene and silver. One is the connection between conjugated pi bond

27   and silver (π-complexation), and the other one is the connection between sulfur and silver

28   (S-metal bond). This is also the main reason that benzene has the competitive adsorption

29   behavior on thiophene.

30   **Keywords:** thiophene, adsorption, desulfurization, Ag/γ-Al$_2$O$_3$ sorbent, adsorption

31   mechanism

32   **1. Introduction**

33   Benzene is an important chemical feedstock, which is widely used for synthesizing of

34   polymer[1], resin[2], fiber[3], pharmaceuticals, pesticides, explosives, dyes and so on. But as its

35   main source, the coking benzene contains a certain content of sulfur-containing compounds,

36   especially thiophene, which will have bad effects on further uses of benzene[4]. Accordingly,

37   the attempts have been made for the purification of coking benzene and some methods to

38   chemically remove thiophene impurities from benzene have been presented. Nowadays, the

39   methods industrialized for the benzene desulfurization purification mainly include the sulfuric

40   acid washing, the catalytic hydrogenation and the extractive rectification. However, the

41   sulfuric acid refining method has the disadvantages of equipment corrosion and

42   environmental pollution[5], the catalytic hydrogenation method consumes hydrogen and has

43   high operating costs, the extractive rectification method consumes large amount of energy and

44   desulfurization efficiency is not very high[6]. In contrast, selective adsorption method has the

45   great potential with the advantages of smaller equipment corrosion, less environmental

46   pollution, lower operating costs, and no hydrogen consumed.

47   However, lots of literature about selective adsorption method are all almost focused on the

48 desulfurization in the transportation fuels[7-15], only a few on the purification of benzene[16-19].

49 Some researchers reported that the transition metal-based sorbent is effective for selectively

50 adsorbing the sulfur compounds in the liquid hydrocarbon fuels at ambient temperature under

51 atmospheric pressure with low investment and operating cost[20]. Transition metal (Cu, Zn, Ni

52 or Ag) could enhance adsorption properties for thiophene and toluene on some sorbents, such

53 as Y-zeolites[21, 22], because Cu and Ag in sorbents are likely combine S-containing compounds

54 by π-complexation[23], Ni and Zn in the S-sorb desulfurization catalyst invented by Sinopec

55 and Philips companies play a very important role on the desulfurization process[24, 25].

56 Nevertheless, a common problem is that the aromatic compounds, e.g. benzene, have the

57 competitive adsorption with thiophene[8, 26, 27], because benzene has very similar physical and

58 chemical properties as that of thiophene, and thus have an obvious competitive effect on

59 thiophene adsorption. Therefore, most of these sorbents reported for desulfurization of liquid

60 fuel could not remove enough thiophene from benzene to give the required low sulfur

61 concentration because the adsorptive removal of thiophene from liquid fuel and benzene is

62 quite different. For liquid fuel, its main components are saturated hydrocarbons, the

63 competitive effect of which is much less and can be ignored, whereas for conking benzene,

64 the main component is benzene. Even though there is the study about the competitive

65 adsorption of thiophene and benzene[28], it is only the removal of thiophene from fuel

66 containing the similar level of benzene, in which the competitive adsorption is much smaller

67 comparing with benzene solvent. Therefore, it is difficult to remove thiophene with the ppm

68 level from benzene because of the competitive adsorption of aromatic compound with very

69 similar physical and chemical properties. In order to improve the sulfur capacity and

70 efficiency of sorbents removing thiophene from benzene, it is necessary to study their

71 adsorption mechanism and optimize the technological parameters.

72   In this paper, γ-Al_2O_3 was selected as the support and different metal nitrates were chosen

73 as the precursors of active components because of their high water solubility and the easy

74 decomposition during heating. A series $M/\gamma-Al_2O_3$ sorbents were prepared by incipient

75 wetness impregnation method. And then the removal of thiophene from benzene was

76 investigated. In order to investigate the adsorption mechanism of thiophene on $M/\gamma-Al_2O_3$

77 sorbent, the adsorption behaviors of the aromatic hydrocarbon (benzene) and the unsaturated

78 cyclic sulfur organic-compound (thiophene) and their saturated analogs (cyclohexane and

79 tetrahydrothiophene, respectively) on $M/\gamma-Al_2O_3$ sorbent were compared.

80 **2. Experimental**

81 *2.1. Preparation of sorbents*

82 $\gamma-Al_2O_3$ powder (0.177–0.125 mm), a meso-pore material, which was purchased from

83 Shandong Kunpeng New Materials Co. Led., was used as the support of sorbent. Before use,

84 it was dried at 120 °C for 4 h to remove the water. Then, it was respectively incipient wetness

85 impregnated in the aqueous solution of $Cu(NO_3)_2$, $Ni(NO_3)_2$, $Zn(NO_3)_2$ and $AgNO_3$ with a

86 predicted volume for 4 h. The samples prepared were dried at 80 °C for 2 h, calcined in

87 Muffle furnace at 500 °C for 4 h to obtain the experimental sorbents.

88 The actual silver loading amount of the prepared samples was quantified using the Volhard

89 method. The samples were first dried overnight at 220 °C, and dissolved with excess HNO_3

90 and titrated with a standard thiocynate solution with an Fe(III) indicator. And the amount of

91 copper, nickel and zinc loaded on $\gamma-Al_2O_3$ was analyzed by atomic absorption

92 spectrophotometer (AAS). The series sorbents prepared and their metal loaded amounts were

93 shown in **Table 1**. A0 denotes the blank $\gamma-Al_2O_3$ support, which is the original $\gamma--Al_2O_3$

94 following the sorbent preparation procedure without adding any metal. A5, A10, A15 and

95 A20 respectively denote the sorbent with different Ag content. C5, N5, Z5 denote the sorbent

96 with Cu, Ni and Zn as the active component respectively.

97

98

99   **Table 1.** The metal content of series prepared sorbents

Sorbents	A0	A5	A10	A15	A20	C5	N5	Z5
Metal content (wt%)	0.0	4.6	9.5	13.8	17.6	4.7	4.4	4.5

100

101   *2.2. Adsorption experiments*

102

In order to choose the suitable active component for thiophene adsorption from benzene，

103 1.00 g of A0, A5, C5, N5 and Z5 sorbent was respectively soaked in 4.00 mL

104 thiophene-benzene solution with the thiophene concentration of 559.8 mg/L in an ampoule

105 bottle at room temperature for 24 h, which was considered that it reached the adsorption

106 quasi-equilibrium and also was proved by the data stated in this paper. After adsorption, the

107 concentration of thiophene in the solution was determined by gas chromatography GC-950

108 (Shanghai Haixin chromatography Co., Ltd.) coupled with flame photometric detector (FPD)

109 and TCEP-7 column (2.5 m $\times$ ϕ4 mm), and the column temperature, inlet temperature and

110 detector temperature are 80 °C, 120 °C and 160 °C, respectively. The carrier gas is high purity

111 nitrogen, and the column pressure is 0.1 Mpa. The flow rate of high purity hydrogen and air

112 for FPD is 40 mL/min and 50 mL/min, respectively.

113   In order to investigate the influence of active metal component on thiophene adsorption and

114 the corresponding adsorption mechanism, the sorbents with different active component and

115 different content were put in 4.00 mL different organic sulfur-containing solutions shown in

116 **Table 2** at room temperature for 24 h. The reason why these sulfur-containing solutions were

117 used is: thiophene molecule has a conjugated pi bond and a sulfur atom, tetrahydrothiophene

118 molecule has a sulfur atom but does not have a conjugated pi bond, benzene molecule has a

119 conjugated pi bond but does not have a sulfur atom, cyclohexane has no conjugated pi bonds

120 and sulfur, and the structure diagram of those four compounds was shown in **Figure 1**. The

121   desulfurization efficiency for the sulfur-containing compounds in different solution on the

122   selected sorbent was measured. The effect of the conjugated pi bond on adsorption can be

123   explored by comparing the desulfurization efficiency in thiophene-benzene solution (TH-B)

124   and thiophene-cyclohexane solution (TH-C). The effect of the sulfur atom on adsorption can

125   be explored by comparing the desulfurization efficiency in thiophene-benzene solution (TH-B)

126   and   tetrahydrothiophene-benzene   solution   (THT-B).   While,

127   tetrahydrothiophene-thiophene-benzene   solution   (TH-THT-B)   and

128   tetrahydrothiophene-thiophene-cyclohexane solution (TH-THT-C) were used to further

129   explore the adsorption mechanism.

130   **Table 2.** Solutions used in this study

Solutions	sulfur-containing compounds	Solvent	$C_{thiophene}$ (mg/L)	$C_{tetrahydrothiophene}$ (mg/L)
TH-B	thiophene	benzene	559.8	0.0
THT-B	tetrahydrothiophene	benzene	0.0	592.1
TH-C	thiophene	cyclohexane	592.5	0.0
TH-THT-B	thiophene/tetrahydrothiophene	benzene	545.2	592.1
TH-THT-C	thiophene/tetrahydrothiophene	cyclohexane	543.9	577.6

131

132
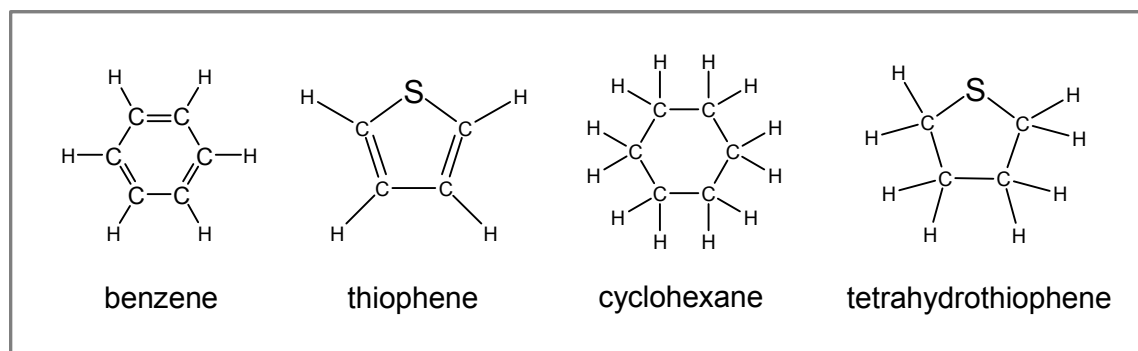
133   **Figure 1** Structure diagram of benzene, thiophene, cyclohexane and tetrahtdrothiophene

134   The desulfurization efficiency (η, %) and thiophene adsorption capacity (Q, mg/g sorbent)

135   were calculated as equations (1) and (2).

136    $$\eta = \frac{c_0 - c}{c_0} \times 100\%$$ **(1)**

137    $$Q = \frac{4 \times (c_0 - c)}{1000}$$ **(2)**

138   where, c_o is the initial concentration of thiophene or tetrahydrothiophene in the solution

139   (mg/L); c is the concentration of thiophene or tetrahydrothiophene in the solution (mg/L)

140   when it reached the adsorption quasi-equilibrium.

141   The saturation adsorption capacities, measured my weight method, for benzene, thiophene

142   and hydrotetrathiophene of A15 sorbent are 19.36mg/g, 24.66 mg/g and 36.51mg/g. The best

143   sorbent was put into 4.00 mL thiophene, tetrahydrothiophene and benzene with the

144   analytically pure at room temperature for 24 h respectively, then filtrated and dried in a

145   vacuum oven at 50 °C for 12 h, and the samples prepared were denoted by A15TH, A15THT

146   and A15B respectively.

147   *2.3. Characterization of sorbents*

148   The structure of sorbents was characterized by X-ray diffraction (XRD) apparatus of

149   D/max-rB, which was made in Janpan, at a scanning rate of 5 °/min from 30 ° to 80 ° with

150   Cu-Kα radial, λ=0.15046 nm X-ray, 40 kV tube voltage and 100 mA tube current. The

151   surface area, pore volume and pore size distribution of the samples were measured by

152   nitrogen adsorption isotherms using a Micromeritics/ASAP2000 apparatus according to the

153   BET and BJH models.

154   FT-IR spectra of samples were recorded on an Equinox55 spectrometer (Bruker, Germany)

155   in the wavenumber range of 400-4000 cm^{-1}, 16 scans were taken at a resolution of 4 cm^{-1}. To

156   prepare pellets, 1mg samples were first ground to powder in an agate mortar and then mixed

157   with 100 mg KBr. A hydraulic press was used to press the resulting mixtures to discs of 10

158   mm in diameter at 10 MPa for 2 min.

159   **3. Results and discussion**

160   *3.1. Selection of active component for desulfurization over prepared M/γ-Al₂O₃ sorbents*

161   **Figure 2** shows the desulfurization efficiencies and thiophene adsorption capacity of

162   sorbents with different metal components in thiophene-benzene solution. It can be seen that

163   A0 sorbent which is the blank sample, γ-Al$_2$O$_3$ support without metal loaded actually, can

164   only adsorb a little thiophene (0.006 mg/g) from benzene with the desulfurization efficiency

165   of 2.9%, whereas the desulfurization efficiency of other sorbents with metal loaded (C5, N5,

166   Z5 and A5) is significantly higher. This indicates that the metals (Cu, Ni, Zn and Ag) loaded

167   on γ-Al$_2$O$_3$ are the main active components, which play a very important role on thiophene

168   adsorption, and the activity of silver is the highest. It was reported in the literature that after

169   modification γ-Al$_2$O$_3$ in Cu(NO$_3$)$_2$, Ni(NO$_3$)$_2$ or Zn(NO$_3$)$_2$ aqueous solution followed by

170   calcination in air, these metal elements will exist as their oxidates[29], which belong to Lewis

171   acid. In contrast, thiophene is soft Lewis base[30], thus thiophene can combine with such metal

172   oxidates. Moreover, NiO, ZnO, and CuO are intermediate Lewis acids, whereas Ag and Ag$_2$O

173   are both soft Lewis acid. So Ag and Ag$_2$O has a stronger force with thiophene according to

174   the principle of "Hard and Soft Acid and Base"－hard likes the hard and soft likes the soft[31].

175   This could explain Ag component is more suitable for the preparation of M/γ-Al$_2$O$_3$ sorbent

176   for the desulfurization from coking benzene, compared with Cu, Ni and Zn.
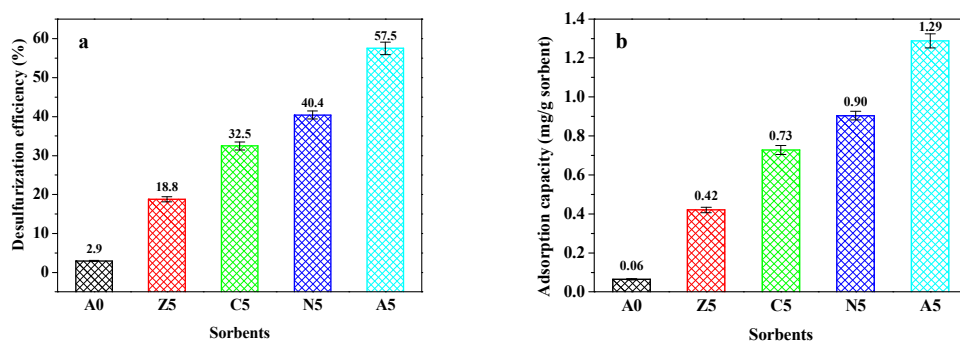
177

178   **Figure 2.** Desulfurization efficiency (a) and thiophene adsorption capacity (b) of sorbents

179   with different metal loaded in TH-B solution

180   **3.2.** *Effect of loading amount and distribution of metal component on desulfurization activity*

181   *of sorbent*

182   From above experimental results, the desulfurization activity of Ag/γ-Al$_2$O$_3$ sorbent is

183   higher than others. So it is necessary to investigate the effect of loading amount and

184   distribution of silver on desulfurization activity of Ag/γ-Al$_2$O$_3$ sorbent. **Figure 3** illustrates the

185   desulfurization efficiency and thiophene adsorption capacity of Ag/γ-Al$_2$O$_3$ sorbents with

186   different silver loaded amount in thiophene-benzene solution. It can be found that from A0

187   sorbent to A15 sorbent, the desulfurization efficiency and thiophene adsorption capacity

188   increase with the increase of silver content (shown in **Table 1**). However, compared with A15

189   sorbent, the silver content of A20 sorbent is higher, but its desulfurization efficiency (30.6%)

190   is much lower than that of A15 sorbent (96.9%). In order to reveal this phenomenon, XRD,

191   SEM/EDS and N$_2$ adsorption were carried out to characterize sliver existing form and

192   distribution and the physical structure of A0, A5, A10, A15 and A20 sorbents, which are the

193   typical properties affecting the desulfurization activity of sorbent.
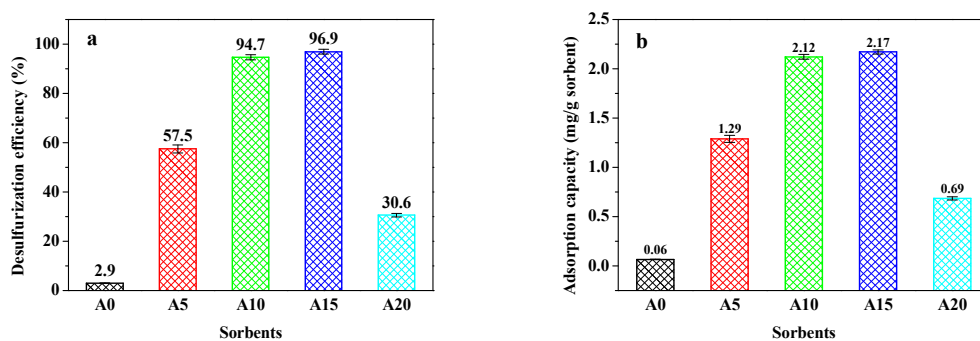
194

195   **Figure 3.** Desulfurization efficiency and thiophene adsorption capacity of Ag/γ-Al$_2$O$_3$

196   sorbents with different silver content in TH-B solution

197   XRD patterns of Ag/γ-Al$_2$O$_3$ sorbents with different Ag content are displayed in **Figure 4**.

198   Three diffraction peaks at 37.28 °, 46.28 ° and 67.03 ° corresponding to γ-Al$_2$O$_3$, indicates

199   that the crystal structure of γ-Al_2O_3 is retained after $AgNO_3$ loaded and followed heat

200   treatment. Other peaks at 38.12 °, 44.30 °, 64.44 ° and 77.40 °, corresponding to the simply

201   Ag^0 crystals[32], show that the active component mainly appears in the form of Ag^0 after

202   calcination step during preparation. **Figure 5** shows the thermal decomposition process of

203    $AgNO_3$ in air. The decomposition begins at about 450 °C, which is the same as the result

204   reported by literature[29], and when the decomposition finished, about 64% of the total weight

205   left, which is just the silver content in pure $AgNO_3$. So from this point, $AgNO_3$ loaded on

206   sorbent should be decomposed under the experimental condition (calcinations temperature

207   was 500 °C) and the chemical reaction follows the equation of $2AgNO_3 = 2Ag+O_2+2NO_2$[33, 34].

208   In order to further investigate the silver existing form, FT-IR was carried out to characterize

209   A15 sorbent. As shown in **Figure 6**, for A15 sorbent, its XPS spectral of the core level of

210   both Ag 3d$_{3/2}$ (a) and O 1s all could be deconvoluted into three peaks. As demonstrated in

211   **Figure 6(a)**, in the XPS spectral of Ag 3d3/2, the peaks at 373.7 eV, 374.6 eV and 375.5 eV are

212   corresponding to Ag^0 [35, 36], Ag_2O and Ag-O-Al species, respectively. As listed in **Figure 6(b)**,

213   n the XPS spectral of O1s the peak at 530.6 eV is attributed to Al_2O_3, and the peaks at 532.2 eV

214   and 533.0 eV should belong to Ag_2O and Ag-O-Al species, respectively. As listed in **Figure 7**,

215   in the spectrum of A0, the peaks at 3438 cm^{-1} and 1636 cm^{-1} are attributed to -OH groups, the

216   peaks at 760 cm^{-1} and 574 cm^{-1} belong to O-Al bond, whereas in the spectrum of A15, the

217   intensity of peaks at 2955 cm^{-1}, 2926 cm^{-1} and 2855 cm^{-1} are obviously increases, and some

218   new peaks, 1385 cm^{-1}, 1385 cm^{-1} and 1116 cm^{-1} appear, which are attributed to Ag_2O, and the

219   peak at 1743 cm^{-1} may be corresponding to Ag-O-Al. The XRD, XPS and FT-IR results all

220   suggest that silver exists in Ag0, Ag_2O and Ag-O-Al forms on γ-Al_2O_3 support, and among of

221   them Ag is the main component.
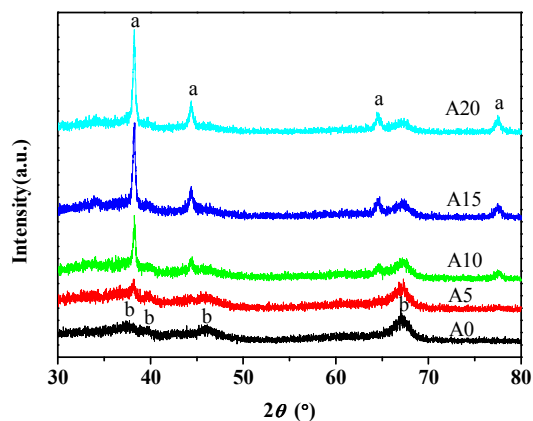
222

223   **Figure 4.** XRD patterns of Ag/γ-Al$_2$O$_3$ series sorbents prepared (a: Ag, b: γ-Al$_2$O$_3$)
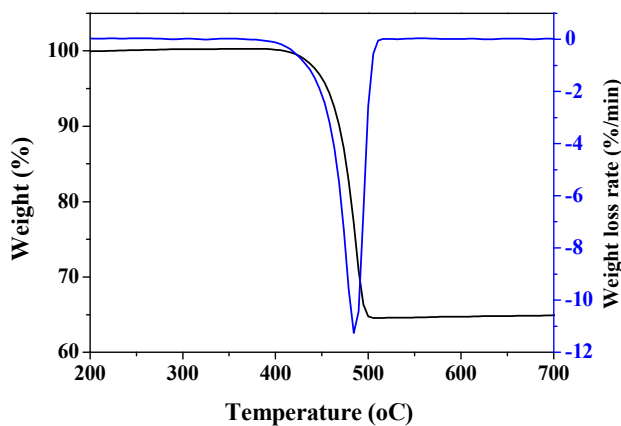
224

225   **Figure 5.** TG and DTG curves of AgNO$_3$ in air
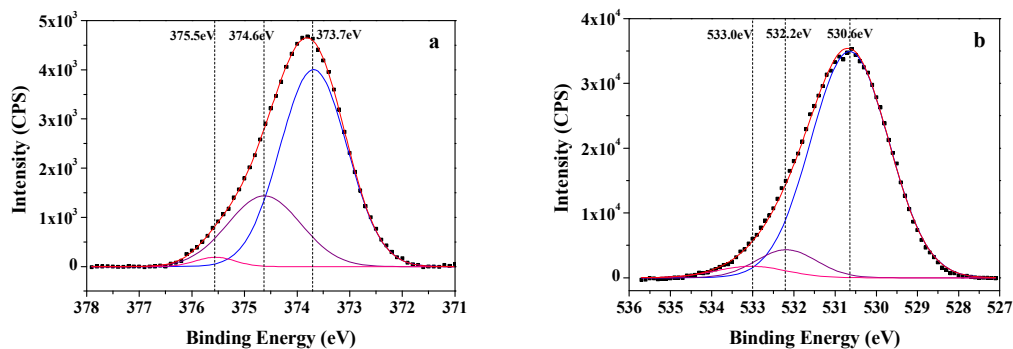
226

227   **Figure 6.** XPS spectral of the core level of Ag 3d3/2 (a) and O 1s region recorded

228   with A15 sorbent

229
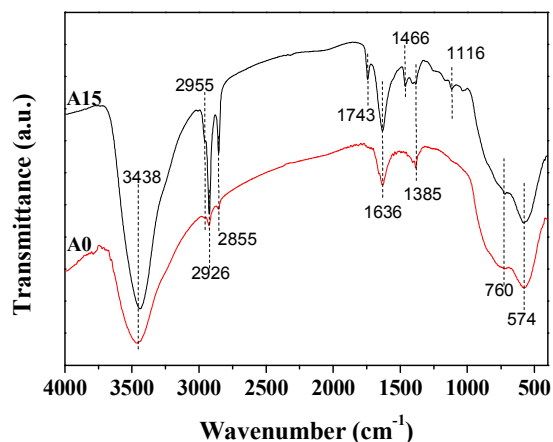
Figure 7. FT-IR spectral of A0 and A15 sorbents

231   Silver distribution on the surface of Ag/γ-Al$_2$O$_3$ sorbents was measured by SEM/EDS, and

232   the results are shown in **Figure 8**. On the surface of A10 sorbent, silver distributes

233   homogeneously, and there is no sliver agglomeration in the surface EDS image, which could

234   explain the relative high desulfurization efficiency of A10 sorbent. On A15 sorbent's surface,

235   most of sliver is still distributed very well which should explain why the desulfurization

236   efficiency of A15 sorbent is higher than that of A10 sorbent. Moreover, a few small

237   particles ,which are the sliver agglomeration verified from the EDS results, appear on A15

238   sorbent could explain why the desulfurization efficiency increment from A10 to A15 is not so

239   obvious as that from A5 to A10. This should explain why the desulfurization efficiency of

240   A15 sorbent is slightly higher than that of A10 sorbent. However, for A20 sorbent, most of its

241   surface was covered by sliver agglomeration particles, which could aromatically decrease its

242   desulfurization efficiency, and this is why the desulfurization activity of A20 sorbent is much

243   lower than that of A15 sorbent.

244

245

246

Sorbents	SEM and EDS images	Surface EDS images
A10		
A15		
A20		
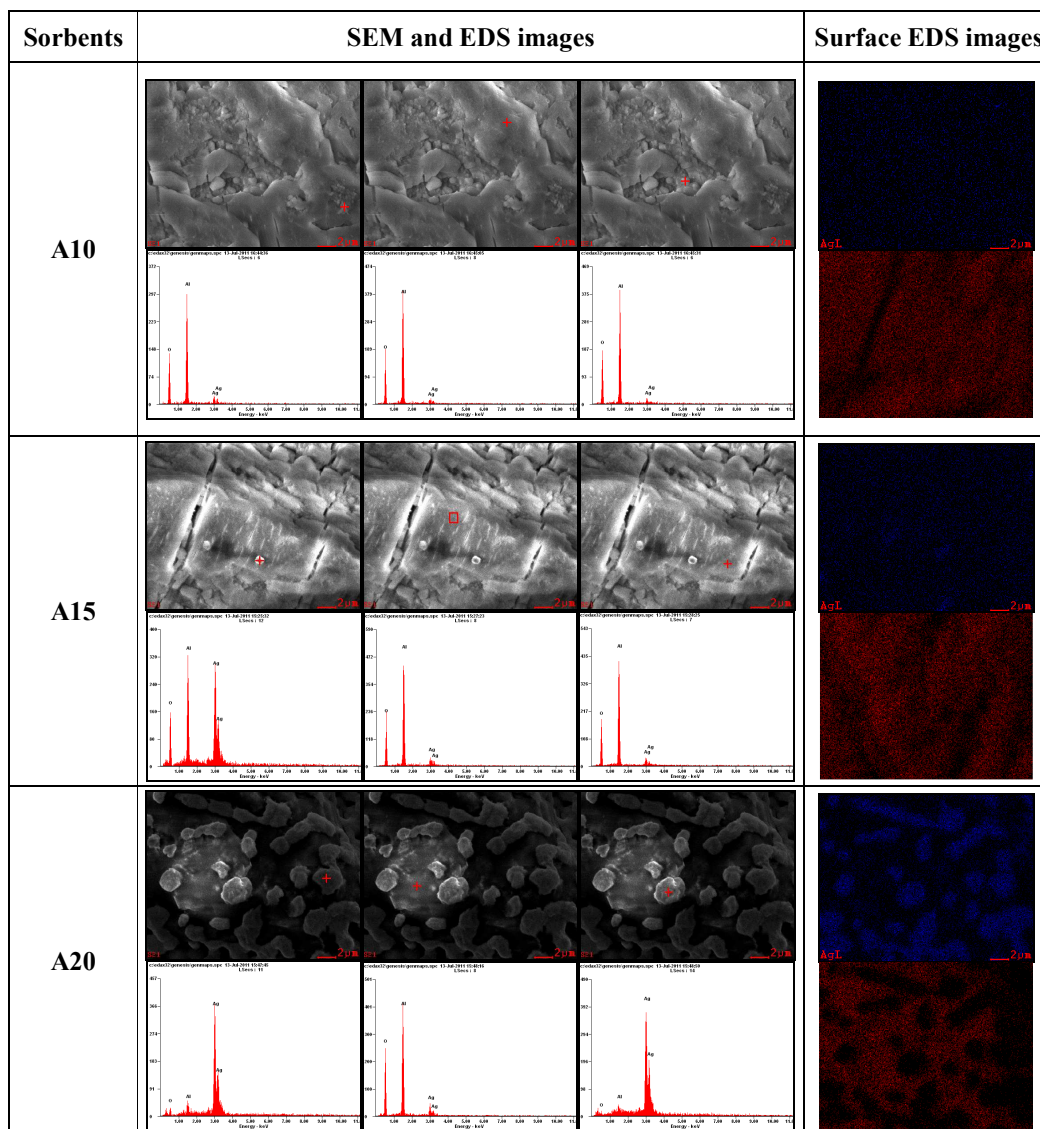
Figure 8. SEM and EDS results of A10, A15 and A20 sorbents

Figure 9 provides the nitrogen adsorption and desorption isotherms of sorbents. The adsorption isotherms of all the sorbents belong to the typical IV type, and all sorbents have mesoporous adsorption behavior. In adsorption isotherms, as the relative pressure increasing from 0.4 to 0.7, the curves rises up sharply, which can be attributed to the occurrence of capillary condensation. And in adsorption/desorption branches, a hysteresis loop is appeared, which indicates the mesopore characteristic of the adsorption-desorption isotherms. The corresponding surface area and pore size distribution of Ag/γ-Al$_2$O$_3$ sorbents are respectively listed in **Table 3**. The pore volume and BET specific area (S$_{BET}$) of Ag/γ-Al$_2$O$_3$ sorbents all

256 decreases with the silver content increasing. The decrease of S_{BET} for the A20 sorbent with

257 20% Ag content should be due to the agglomeration of the active component, which can be

258 observed in its SEM/EDS image (**Figure 8**), and this is also why the total pore volume and

259 the average pore diameter (shown in **Table 3**) of A20 sorbent is much less than that of A15

260 sorbent.
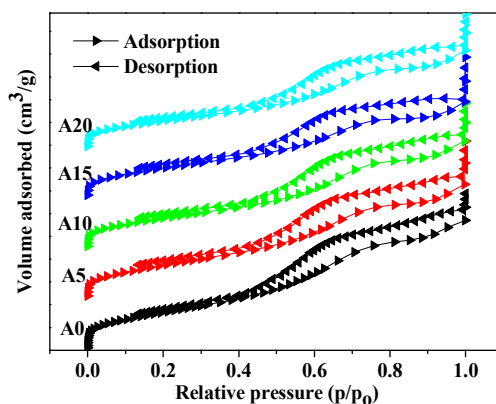
261

262 **Figure 9.** N_2 adsorption and desorption isotherms of Ag/γ-Al_2O_3 sorbents

263 **Table 3.** Surface area and pore volume of different sorbents

Sorbents	Specific surface area (m^2/g)	Pore volume (cm^3/g)	Average pore diameter (nm)
A0	156	0.208	36.8
A5	146	0.180	35.0
A10	132	0.170	33.5
A15	132	0.154	31.5
A20	120	0.145	27.9

264 *3.3. Adsorption desulfurization mechanisms of Ag/γ-Al₂O₃ sorbent*

265 Adsorption results of Ag/γ-Al_2O_3 sorbents in TH-B and TH-C solutions are shown in

266 **Figure 10**. In TH-C solution, the desulfurization efficiency of all these Ag/γ-Al_2O_3 sorbents is

267 about 100%, whereas, in TH-B solution, it is lower for A10 and A15 sorbents, and much

268 lower for A5 and A20 sorbents. This suggests that benzene presents the competitive

269 adsorption with thiophene over Ag/γ-Al_2O_3 sorbent. This competitive adsorption effect should

270   be attributed to the connection between the active component and the conjugated pi bond as

271   well as the π-complexation, because the structures of thiophene and benzene are very similar

272   to each other with the unsaturated organic compounds, and the similar composition of six

273   electron conjugated pi bond, which could connect to silver on these sorbents by

274   π-complexation. However, for cyclohexane, it does not have conjugated pi bond, and thus

275   does not have competitive adsorption effect, which is why the desulfurization efficiency of all

276   the Ag/γ-Al$_2$O$_3$ sorbents is close to 100%.
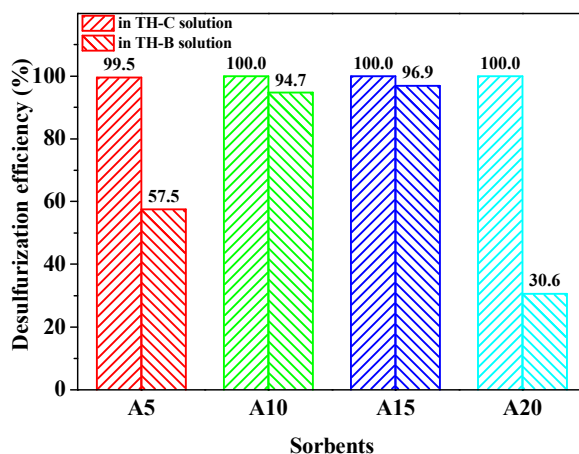
277

278   **Figure 10.** Comparison of desulfurization efficiency of different Ag/γ-Al$_2$O$_3$ sorbents in

279   TH-B and TH-C solutions

280   **Figure 11** shows the desulfurization efficiency of Ag/γ-Al$_2$O$_3$ sorbents in TH-B and THT-B

281   solutions. It can be found that the desulfurization efficiency of all the Ag/γ-Al$_2$O$_3$ sorbents in

282   THT-B solution is higher than that in TH-B solution, which means that the removal of

283   tetrahydrothiophene from benzene is much easier than that of thiophene from benzene, and

284   the removal efficiency of tetrahydrothiophene from benzene over Ag/γ-Al$_2$O$_3$ sorbents is

285   around 99%. It indicates that benzene almost has no competitive adsorption effect on the

286   adsorption of tetrahydrothiophene on Ag/γ-Al$_2$O$_3$ sorbents' surface even benzene could

287   connect to silver by π-complexation, which means that tetrahydrothiophene molecule could

288   be adsorbed on Ag/γ-Al$_2$O$_3$ sorbents by a different way. And thus, in addition to the

289   π-complexation adsorption mechanism discussed above, there should be another adsorption

290   mechanism between thiophenes and silver. If a comparison is made between

291   tetrahydrothiophene and thiophene molecules, it is very easy to find that both of them all have

292   sulfur atoms, which have lone-pair electrons. So it is probable that tetrahydrothiophene and

293   thiophene can act as the n-type donors by donating the lone-pair electrons that lie in the plane

294   of the ring to the silver on Ag/γ-Al$_2$O$_3$ sorbents to form S-Ag bond (S-M mechanism[37]),

295   because silver has unoccupied orbital, which could accept this donation.
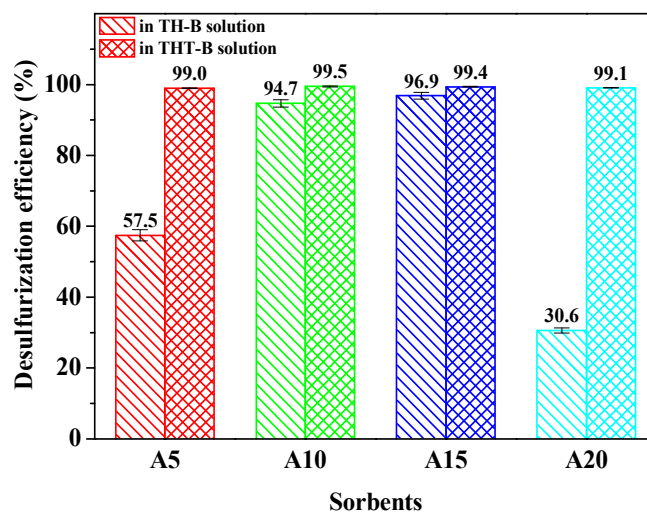
296

297   **Figure 11.** Desulfurization efficiency of Ag/γ-Al$_2$O$_3$ sorbents in TH-B and THT-B solutions

298   **Figure 12** show the FT-IR spectral of different samples in the range of 4000 cm^{-1}-400

299   cm^{-1} (a), 3100 cm^{-1}-2700 cm^{-1} (b) and 1800 cm^{-1}-1000 cm^{-1} (c). It can be seen that, after

300   benzene, thiophene and tetrahydrothiophene absorbed on A15 sorbent, the intensity of the

301   peaks at 2925 cm^{-1}, 2926 cm^{-1}, 2855 cm^{-1} and 1385 cm^{-1} all decreased significantly, and the

302   peaks at 1743 cm^{-1}, 1462 cm^{-1}, 1116 cm^{-1} disappeared, which suggest that the Ag$_2$O and

303   Ag-O-Al spices all can combine to benzene, thiophene and tetrahydrothiophene.
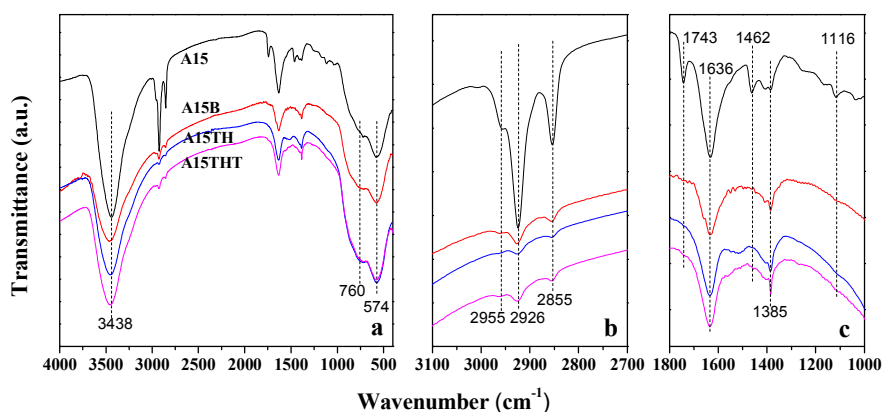
Figure 12. FT-IR spectral of different samples in the range of 4000 cm^{-1}-400 cm^{-1} (a), 3100 cm^{-1}-2700 cm^{-1} (b) and 1800 cm^{-1}-1000 cm^{-1} (c)

In order to further understand the π-complexation and S-M mechanisms proposed above, the desulfurization behavior in TH-THT-C and TH-THT-B solutions over Ag/γ-Al$_2$O$_3$ sorbents was studied, and the results were shown in **Figure 13**. The desulfurization efficiency for tetrahydrothiophene and thiophene in TH-THT-C solution is 100%, whereas that for thiophene in TH-THT-B solution (95.8%) is relatively lower. It indicates that thiophene almost has no competitive effect on tetrahydrothiophene adsorption, which may because the S-Ag bond formed between tetrahydrothiophene and silver is stronger than that formed between thiophene and silver, for the sulfur atom in tetrahydrothiophene molecule has two lone-pair electrons, whereas the sulfur atom in thiophene molecule only has one lone-pair electrons. It could also explain why the adsorption rate of tetrahydrothiophene (shown in **Figure 14**) in these two solutions is much higher than that of thiophene.

318
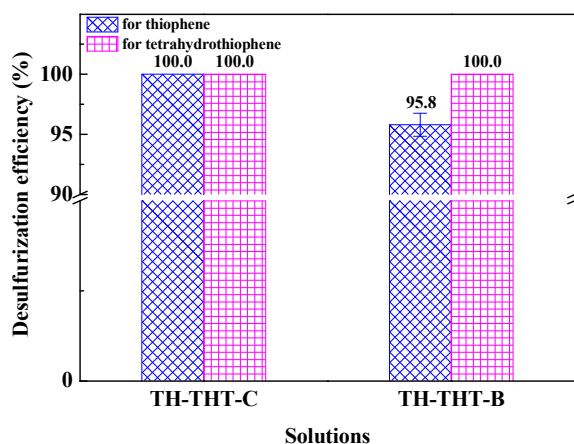
Figure 13. Comparison of thiophene adsorption over A15 sorbent in TH-THT-B and

320 TH-THT-C solution

321
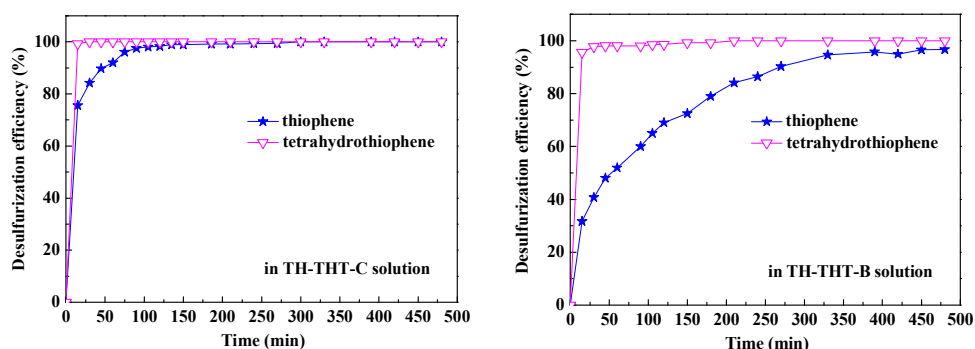
Figure 14. Adsorption curves of thiophene and tetrahydrothiophene over A15 sorbent in

323 thiophene-tetrahydrothiophene-cyclohexane and thiophene-tetrahydrothiophene-benzene

324 solutions

4. Conclusions

326 Copper, nickel, zinc and silver elements loaded on γ-Al$_2$O$_3$ could significantly improve the

327 desulfurization activity of M/γ-Al$_2$O$_3$ sorbents, and silver is the best. On Ag/γ-Al$_2$O$_3$ sorbent,

328 the loading amount and distribution of silver are the main factors influencing the

329 desulfurization capacity of sorbent. With the increase of silver content in sorbent from 0 to

330 13.8%, the desulfurization efficiency increases, whereas when it is increased to 17.6%, the

331 sliver agglomeration appears very seriously, and thus its desulfurization efficiency decreases

332 obviously. There are two adsorption desulfurization mechanisms on Ag/γ-Al$_2$O$_3$ sorbent,

333 π-complexation and S-M bond between thiophene and silver. The competitive adsorption of

334 benzene with thiophene over Ag/γ-Al$_2$O$_3$ sorbent is caused by the π-complexation

335 mechanism.

336 **Acknowledgements**

342 **References**

343   1.   P. F. McMillan, *Nat Mater*, 2007, 6, 7-8.

344   2.   R. Ruhela, A. Rao, N. Iyer, A. Das, P. Kumar, A. K. Singh, B. S. Tomar and R. C. Hubli, *RSC Advances*,
345   2014, 4, 62654-62661.

346   3.   T. Fukuda, Y. Hayasaki, T. Hasumura, Y. Katsube, R. L. D. Whitby and T. Maekawa, *RSC Advances*,
347   2015, 5, 12671-12677.

348   4.   J. Liao, Y. Wang, L. Chang and W. Bao, *Green Chemistry*, 2015, 17, 3164-3175.

349   5.   *United States Pat.,* 2707699, 1955.

350   6.   *United States Pat.,* 3879268, 1975.

351   7.   Y. Shen, X. Xu and P. Li, *RSC Advances*, 2012, 2, 6155-6160.

352   8.   F. Duan, C. Chen, G. Wang, Y. Yang, X. Liu and Y. Qin, *RSC Advances*, 2014, 4, 1469-1475.

353   9.   P. S. Kulkarni and C. A. M. Afonso, *Green Chemistry*, 2010, 12, 1139-1149.

354   10.   X. Li, X. Zhang and L. Lei, *Separation and Purification Technology*, 2009, 64, 326-331.

355   11.   G. Bai, X. Lan, X. Liu, C. Liu, L. Shi, Q. Chen and G. Chen, *Green Chemistry*, 2014, 16, 3160-3168.

356   12.   A. Samokhvalov, E. C. Duin, S. Nair, M. Bowman, Z. Davis and B. J. Tatarchuk, *The Journal of*
357   *Physical Chemistry C*, 2010, 114, 4075-4085.

358   13.   C. Shen, Y. J. Wang, J. H. Xu, Y. C. Lu and G. S. Luo, *Green Chemistry*, 2012, 14, 1009-1015.

359   14.   C. Li, D. Li, S. Zou, Z. Li, J. Yin, A. Wang, Y. Cui, Z. Yao and Q. Zhao, *Green Chemistry*, 2013, 15,
360   2793-2799.

361   15.   T. Jin, Q. Yang, C. Meng, J. Xu, H. Liu, J. Hu and H. Ling, *RSC Advances*, 2014, 4, 41902-41909.

362   16.   Y. Zeng and S. Ju, *Separation and Purification Technology*, 2009, 67, 71-78.

363   17.   L. Song, T. Bu, L. Zhu, Y. Zhou, Y. Xiang and D. Xia, *The Journal of Physical Chemistry C*, 2014, 118,
364   9468-9476.

365   18.   J. Liao, W. Bao, Y. Chen, Y. Zhang and L. Chang, *Energy Sources, Part A: Recovery, Utilization, and*
366   *Environmental Effects*, 2012, 34, 618-625.

367   19.   J. Liao, W. Wang, Y. Xie, Y. Zhang, L. Chang and W. Bao, *Separation Science and Technology*, 2012,

368   47, 1880-1885.

369   20.   L. Duan, X. Gao, X. Meng, H. Zhang, Q. Wang, Y. Qin, X. Zhang and L. Song, *The Journal of Physical*
370   *Chemistry C*, 2012, 116, 25748-25756.

371   21.   A. H. M. S. Hussain, M. L. McKee, J. M. Heinzel, X. Sun and B. J. Tatarchuk, *The Journal of Physical*
372   *Chemistry C*, 2014, 118, 14938-14947.

373   22.   L. Wu, J. Xiao, Y. Wu, S. Xian, G. Miao, H. Wang and Z. Li, *Langmuir*, 2014, 30, 1080-1088.

374   23.   D. Lee, J. Kim, H. C. Lee, K. H. Lee, E. D. Park and H. C. Woo, *The Journal of Physical Chemistry C*,
375   2008, 112, 18955-18962.

376   24.   J. Gislason, *Oil Gas J.*, 2001, 99, 72-72.

377   25.   C. Song, *Catalysis Today*, 2003, 86, 211-263.

378   26.   J. Guo, M. J. Janik and C. Song, *The Journal of Physical Chemistry C*, 2012, 116, 3457-3466.

379   27.   S. Sato, F. Nozaki, S.-J. Zhang and P. Cheng, *Applied Catalysis A: General*, 1996, 143, 271-281.

380   28.   A. J. Hernández-Maldonado and R. T. Yang, *Industrial & Engineering Chemistry Research*, 2003, 42,
381   123-129.

382   29.   S. Yuvaraj, L. Fan-Yuan, C. Tsong-Huei and Y. Chuin-Tih, *The Journal of Physical Chemistry B*, 2003,
383   107, 1044-1047.

384   30.   M. Xue, R. Chitrakar, K. Sakane, T. Hirotsu, K. Ooi, Y. Yoshimura, Q. Feng and N. Sumida, *Journal of*
385   *Colloid and Interface Science*, 2005, 285, 487-492.

386   31.   R. G. Pearson, *Journal of the American Chemical Society*, 1963, 85, 3533-3539.

387   32.   S. Ribeiro, C. M. Granadeiro, P. Silva, F. A. Almeida Paz, F. F. de Biani, L. Cunha-Silva and S. S.
388   Balula, *Catalysis Science & Technology*, 2013, 3, 2404-2414.

389   33.   J.-W. Kwon, S. H. Yoon, S. S. Lee, K. W. Seo and I.-W. Shim, *Bull. Korean Chem. Soc*, 2005, 26,
390   837-840.

391   34.   K. Otto, I. Oja Acik, M. Krunks, K. Tõnsuaadu and A. Mere, *J Therm Anal Calorim*, 2014, 118,
392   1065-1072.

393   35.   S. M. Hosseini, I. A. Sarsari, P. Kameli and H. Salamati, *Journal of Alloys and Compounds*, 2015, 640,
394   408-415.

395   36.   S. W. Han, Y. Kim and K. Kim, *Journal of Colloid and Interface Science*, 1998, 208, 272-278.

396   37.   X. Yan, P. Mei, L. Xiong, L. Gao, Q. Yang and L. Gong, *Catalysis Science & Technology*, 2013, 3,
397   1985-1992.

398
399